STEM CELLS®

TISSUE-SPECIFIC STEM CELLS

Maintenance of Undifferentiated State and Self-Renewal of Embryonic Neural Stem Cells by Polycomb Protein Ring1B

MÓNICA ROMÁN-TRUFERO,[a] HÉCTOR R. MÉNDEZ-GÓMEZ,[b,c] CLAUDIA PÉREZ,[d] ATSUSHI HIJIKATA,[e] YU-ICHI FUJIMURA,[e] TAKAHO ENDO,[f] HARUHIKO KOSEKI,[e] CARLOS VICARIO-ABEJÓN,[b,c] MIGUEL VIDAL[a]

[a]Cell and Developmental Biology, Centro de Investigaciones Biológicas and [b]Molecular, Cellular and Developmental Neurobiology, Instituto Cajal, Consejo Superior de Investigaciones Cientificas (CSIC), Madrid, Spain; [c]Centro de Investigaciones Biomédicas en Red sobre Enfermedades Neurodegenerativas (CIBERNED), Instituto de Salud Carlos III, Madrid, Spain; [d]Anatomy and Histopathology, Facultad de Veterinaria, Universidad de León, Campus Vegazana, León, Spain; [e]Developmental Genetics and [f]Bioinformatics and Systems Engineering Division, RIKEN Research Center for Allergy and Immunology, Yokohama, Japan

Key Words. Ring1B • Polycomb • Stem cell • Neural differentiation • Self-renewal

ABSTRACT

Cell lineages generated during development and tissue maintenance are derived from self-renewing stem cells by differentiation of their committed progeny. Recent studies suggest that epigenetic mechanisms, and in particular the Polycomb group (PcG) of genes, play important roles in controlling stem cell self-renewal. Here, we address PcG regulation of stem cell self-renewal and differentiation through inactivation of Ring1B, a histone H2A E3 monoubiquitin ligase, in embryonic neural stem cells (NSCs) from the olfactory bulb of a conditional mouse mutant line. We show that neural stem/progenitor cell proliferation in vivo and in neurosphere assays is impaired, lacking Ring1B, and their self-renewal and multipotential abilities, assessed as sphere formation and differentiation from single cells, are severely affected. We also observed unscheduled neuronal, but not glial, differentiation of mutant stem/progenitor cells under proliferating conditions, an alteration enhanced in cells also lacking Ring1A, the Ring1B paralog, some of which turned into morphologically identifiable neurons. mRNA analysis of mutant cells showed upregulation of some neuronal differentiation–related transcription factors and the cell proliferation inhibitor Cdkn1a/p21, as well as downregulation of effectors of the Notch signaling pathway, a known inhibitor of neuronal differentiation of stem/progenitor cells. In addition, differentiation studies of Ring1B-deficient progenitors showed decreased oligodendrocyte formation in vitro and enhanced neurogenesis and reduced gliogenesis in vivo. These data suggest a role for Ring1B in maintenance of the undifferentiated state of embryonic neural stem/progenitor cells. They also suggest that Ring1B may modulate the differentiation potential of NSCs to neurons and glia. STEM CELLS *2009;27:1559–1570*

Disclosure of potential conflicts of interest is found at the end of this article.

INTRODUCTION

The generation of cell lineages during development and the integrity of tissues in the adult depends on a variety of self-renewing embryonic and adult stem cells [1]. Self-renewal allows the maintenance of pools of stem cells needed for appropriate embryo development and cell replacement during an organism's life span [2]. Stem cell self-renewal combines the ability to proliferate with the preservation of developmental potential [3]. Embryonic stem (ES) and fetal stem cells proliferate extensively, in contrast to adult stem cells, which proliferate rather sparsely and rely on transit-amplifying progenitors for cell expansion [1, 4]. Developmental potential is maximal in ES cells (pluripotent), whereas other embryonic/fetal and adult stem cells show lineage-restricted potential [1, 5].

Studies on ES cells show that self-renewal is determined by a regulatory network of transcription factors acting together with chromatin regulators, thus defining a cell type–specific epigenetic landscape [6–9]. Among epigenetic regulators, the Polycomb group (PcG) of genes encodes subunits of chromatin complexes (Polycomb repressing complexes [PRCs]). Two of these subunits are endowed with chromatin-

Author contributions: M.R.-T.: collection and/or assembly of data, data analysis and interpretation; H.M.-G.: collection and/or assembly of data, data analysis; C.P.: collection and assembly of data; A.H.: data analysis; Y.F.: collection and assembly of data; T.E.: data analysis; H.K.: provision of study material or patients; C.V.-A.: conception and design, data analysis and interpretation, manuscript revision, financial support; M.V.: conception and design, data analysis and interpretation, financial support, manuscript writing and final approval of manuscript; C.V.-A. and M.V. contributed equally to this work.

Correspondence: Miguel Vidal, Ph.D., Cell and Developmental Biology, Centro de Investigaciones Biológicas, CSIC, Ramiro de Maeztu 9, 28040 Madrid, Spain. Telephone: 34 918373112; Fax: 34 915360432; e-mail: mvidal@cib.csic.es; or Carlos Vicario-Abejón, Ph.D., Molecular, Cellular and Developmental Neurobiology, Instituto Cajal, CSIC, Avda. Doctor Arce 37, 28002 Madrid, Spain. Telephone: 34 915854721; Fax: 34 915854754; e-mail: cvicario@cajal.csic.es Received August 6, 2008; accepted for publication March 12, 2009; first published online in STEM CELLS *EXPRESS* April 2, 2009. 1066-5099/2009/$30.00/0 doi: 10.1002/stem.82

modifying activities. One, Ezh2, is a methyltransferase that modifies lysine 27 of histone H3 [10], whereas Ring1B and its paralog Ring1A are E3 monoubiquitin ligase that modify lysine 119 of histone H2A [11]. Both enzymatic activities belong in nonoverlapping core protein complexes unique to a variety of biochemical entities grouped as PRC2 (H3K27 methyltransferase) and PRC1 (H2AK119 monoubiquitin ligase) [12]. These histone modifications are commonly found on transcriptionally silent loci [13–16]. Currently, it is accepted that PRC2 acts as an instructed chromatin-modifying module [17], whereas PRC1 acts as a reader device that binds to H3K27 methylated nucleosomes [10, 18], although sometimes PRC1 subunits are also recruited to chromatin in a H3K27-independent manner [19].

The PcG role in stem cell self-renewal is best known for ES cells and hematopoietic stem cells [20]. In ES cells, PcG products act as repressors of transcription factors and of components of signaling modules widely used in the generation of cell lineages that appear during development [13, 15]. Recently, it was shown that PRC2-dependent markers and other epigenetic markers are related to changing transcriptional programs associated with transitions from ES cell–derived neural stem cells (NSCs) to neural progenitors and their differentiated progeny [21]. The impact of PcG regulation on NSC self-renewal is more limited and is derive mostly from the study of loss-of-function models of Pcgf4/Bmi1, a PRC1 subunit that acts as a cofactor in H2A ubiquitylation by Ring1A/Ring1B [22]. Mice lacking Bmi1 have a lower number of adult NSCs whose self-renewal ability is severely impaired [23–25]. Acute inactivation of Bmi1, by short hairpin (sh)RNA-mediated inactivation of embryonic neural stem/progenitor cells also results in defective self-renewal [26]. Both Bmi1-deficient adult and fetal stem/progenitor cells have upregulated inhibitors of cell cycle progression. Although Ring1B and Bmi1 are part of a common regulatory device [22, 27], they also show distinctive activities, as seen, for example, in the adult hematopoietic compartment [28]. Here, we set out to investigate the role of the PcG histone E3 monoubiquitin ligase Ring1B in the self-renewal and differentiation potential of embryonic NSCs. Using a model of conditional inactivation of Ring1B to study self-renewal of NSCs from the fetal olfactory bulb, we show that Ring1B promotes embryonic NSC self-renewal by sustaining their proliferative activity and maintaining their undifferentiated state and developmental potential.

Materials and Methods

Mice

Ring1B conditional knockout, *Ring1A* knockout, and genotyping were described previously [28, 29]. Inducible Cre-expressing mouse lines were *Polr2a::CreERT2* [30] and *Rosa26:CreERT2* [31]. Animal handling procedures were institutionally approved and were in accordance with national and European regulations.

Neural Stem/Progenitor Cell Culture

Reagents for cell cultures were bought from Invitrogen (Carlsbad, CA, http://www.invitrogen.com), Sigma-Aldrich (St. Louis, MO, http://www.sigmaaldrich.com), and PeproTech (Rocky Hill, NJ, http://www.peprotech.com). Embryonic olfactory bulb stem cells (OBSCs) were prepared from the olfactory bulb of 13.5 days postcoitum (dpc) mice. Cells were plated and expanded in Dulbecco's modified Eagle's medium (DMEM)/nutrient mixture F12/insulin, apotransferrin, putrescine, progesterone, and sodium selenite supplemented with fibroblast growth factor (FGF)-2 and epidermal growth factor (EGF) [32]. Proliferation assays were performed in cells growing in the presence of FGF-2 and EGF. Cultures were pulsed with 5′-bromo-2-deoxyuridine (BrdU) for 1 hour before fixation. Differentiation assays were performed after mitogen removal from the cultures. For clonal analysis, OBSC spheres were dissociated into a single-cell suspension and diluted to eight cells/ml in DMEM/F12/N12:OBSC-conditioned medium (1:1). Two hundred μl of this suspension was plated into each well of 96-well plates. One day after seeding, wells containing a single cell were marked and induced to proliferate for 9 days, when the wells were screened for the presence of clonal neurospheres. Differentiated clonally derived secondary spheres were finally fixed and triple immunostained to detect the presence of neurons, astrocytes, and oligodendrocytes [33].

Immunostaining of Cultured Cells

Cells were fixed in 4% paraformaldehyde (PFA) and incubated with antibodies to: Ring1B (1:250 [34]), β-tubulin III (Tuj1, 1:2,000; Covance, Princeton, NJ, http://www.covance.com), glial fibrillary acidic protein (GFAP, 1:800; Millipore, Billerica, MA, http://www.millipore.com), O4 (1:8), microtubule-associated protein 2ab (Map2ab) (1:250; Sigma), neurofilament medium chain (NF-m) (1:400; Encor Biotechnology, Gainesville, FL, http://www.encorbio.com), and BrdU (1:1,000; Becton, Dickinson and Company, Franklin Lakes, NJ, http://www.bd.com). Differentiated clones were triple immunostained with antibodies against β-tubulin III (rabbit antibody diluted 1:2,000; Covance), GFAP (mouse antibody, diluted 1:800; Millipore), and O4 (diluted 1:8). The O4 antibody was obtained from the culture medium of O4-producing hybridoma cells, kindly provided by A. Rodríguez-Peña, Consejo Superior de Investigaciones Cientificas. Appropriate secondary antibodies were used to detect specific signals. Cultures were stained with 2 μg/ml 4′,6-diamino-2-phenylindole (DAPI) to stain the nuclei and allow total cell counting.

A terminal deoxynucleotidyl transferase dUTP nick end labeling (TUNEL) assay was performed following the manufacturer's instructions (Roche Diagnostics, Basel, Switzerland, http://www.roche-applied-science.com).

Immunostaining of Tissue Sections

Embryonic day (E)17.5 mouse embryos were perfused with 4% PFA and embryo heads were postfixed in 4% PFA for 2 hours, cryoprotected with Tissue-Tek (Sakura, Tokyo, Japan, http://www.sakura.com), and then frozen at −80°C. Coronal cryostat sections (14 μm) were immunostained with antibodies against: Ring1B (1:400), phospho-H3 (PH3, 1:1,000; Millipore), Tuj1 (1:2,000), GFAP (1:800), and nestin (mouse monoclonal diluted 1:50; Millipore). The TUNEL assay (Roche's kit) was also performed on cryostat sections. Ring1B and Tuj1 immunohistochemistry was done on 7-μm sections of paraffin-embedded fixed embryos. Binding of anti-Ring1B [34] and anti-Tuj1 antibodies was detected with the avidin–biotin–peroxidase complex method (Peroxidase Elite, Vectastain, and ABC kit; Vector Laboratories, Burlingame, CA, http://www.vectorlabs.com) followed by counterstaining with hematoxylin-eosin. Cryostat sections were also prepared from the OBs of E17.5 embryos from pregnant mice that were injected i.p. with BrdU (100 μg/g) 4 hours before embryos were removed. Sections were double immunostained with antibodies against BrdU (1:200; Abcam, Cambridge, U.K., http://www.abcam.com) and TuJ1 or nestin (rabbit polyclonal, diluted 1:1,000, provided by R. McKay, NIH), followed by appropriate fluorescent secondary antibodies. Some sections were stained with DAPI.

Western Blot Analysis

Cells were lysed in RIPA buffer (10 mM Tris-HCl, pH 7.2; 150 mM NaCl; 1% Triton-100; 0.1% sodium dodecyl sulfate; 1% sodium deoxycholate; 5 mM EDTA, 20 mM NaF and Complete [Roche]). Thirty-five μg of total extract was subjected to SDS-PAGE electrophoresis and posterior immunoblotting following standard procedures. Nitrocellulose membranes were incubated

with antibodies specific for Ring1B [34] and α-tubulin (Sigma, clone B-5-1-2).

Microarray Methods and Gene Ontology Analysis

Total RNA was extracted using the Trizol reagent (Invitrogen) and purified with Qiagen RNeasy separation columns (Qiagen, Hilden, Germany, http://www1.qiagen.com). First-strand cDNA was synthesized and hybridized to Affymetrix GeneChip Mouse Genome 430 2.0 arrays (Affymetrix, Santa Clara, CA, http://www.affymetrix.com) to assess and compare the overall gene expression profiles. The signal intensities of probe sets in each chip were normalized with the gcRMA algorithm [35] implemented in the Bioconductor package (Bioconductor, http://bioconductor.org) to estimate the expression value of each probe set in the chip. The annotation information for the probe sets was obtained from RefDIC (RIKEN Research Center for Allergy and Immunology, http://refdic.rcai.riken.jp) [36], and probe sets having no gene information or matching two or more genes were excluded from the analysis. We considered only probe sets whose expression values varied by twofold or more between Ring1B-deficient cells and control cultures. For 972 up/downregulated genes, gene ontology (GO) term enrichment analysis was performed according to a method described by Draghici et al. [37], with a correction for multiple testing using the false discovery rate (FDR) [38]. Eventually, GO terms with a FDR < 0.05 were selected as functionally enriched terms.

Quantitative Reverse Transcription-Polymerase Chain Reaction

Total RNA was isolated using Trizol (Invitrogen) and the reverse transcription (RT) reaction was carried out using the First Strand Synthesis Kit according to the manufacturer's guidelines (Invitrogen). A quantitative polymerase chain reaction (QPCR) analysis was performed in triplicate using 150 ng cDNA per reaction in an iQ5 with Bio-Rad SYBR-Green (Bio-Rad, Hercules, CA, http://www.bio-rad.com). Gene expression data were analyzed with iQ5 software (Bio-Rad). Sequences of primer pairs for the QPCR were obtained from the Primer Bank [39]: *Hes1*, 6680205a2; *Hes5*, 6754182a1; *Hey1*, 6754188a1; *NeuroD1*, 33563268a1; *Tubb3*, 12963615a1; *Cdkn1a*, 6671726a3; *Ina*, 34328368a1; *Id4*, 13624309a1; *Eomes/Tbr2*, 5738950a1; *Prdm16*, 33186878a2; *Ascl1*, 6678806a1; *Zfhx3/Atbf1*, 6680736a1; *Nr2f2/COUP-TFII*, 6753104a1. Other primers were: *Cdkn2a*, 5′-CGAACTCTTTCGGTCGTACCC-3′(forward) and 5′-CGAATCTGCACCGTAGTTGAGC-3′ (reverse) and *Cdknd*, 5′-CTGAACCGCTTTGGCAAGAC-3′ (forward) and 5′-GCCCTCTCTTATCGCCAGAT-3′ (reverse).

Cell Counts and Statistical Analysis

To determine the number of cultured cells expressing a specific antigen, 10 random fields were counted per coverslip using a 40× objective and fluorescence filters [33]. $PH3^+$ cells and $GFAP^+$ cells were counted in 24 serially cut cryostat sections ($n = 3$ wild-type mice and $n = 3$ $Ring1B^{\Delta/\Delta}$ mice). To count $BrdU^+$ and $TuJ1^+$ cells, confocal images from cryostat sections were taken every micron. The entire image stacks were then analyzed and the cells were counted using ImageJ software (Wayne Rasband, National Institutes of Health, USA). Statistical analysis was performed using Student's *t*-test and Sigma Stat Software (Sigma).

Results

Ring1B Is Required for Proliferation of NSCs

Multipotent self-renewing NSCs can be propagated in cell suspension cultures, where they form cell aggregates known as neurospheres [40]. Under these conditions, survival and expansion of stem and progenitor cells result in populations of undifferentiated cells that retain their ability to differentiate

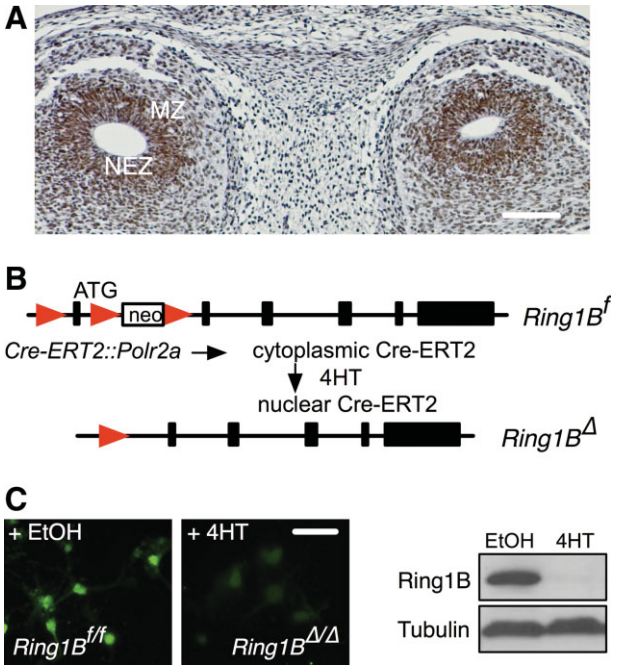

Figure 1. Ring1B expression in the fetal olfactory bulb and strategy for Ring1B inactivation in olfactory bulb stem cells (OBSCs). **(A):** Histochemical analysis of 13.5 days postcoitum olfactory bulb, showing high levels of Ring1B in the neuroepithelial zone (NEZ); some cells located in the mantle zone (MZ) also expressed Ring1B. **(B):** Strategy for generation of $Ring1B^{\Delta/\Delta}$ cells. ATG denotes the initiation codon of Ring1B, red triangles loxP sequences and filled boxes Ring1B exons. **(C):** Ring1B immunostaining (left) and Western blotting (right) analysis of control OBSCs (ethanol [EtOH]) and $Ring1B^{\Delta/\Delta}$ OBSCs (hydroxytamoxifen, [+4HT]) shows almost total deletion of Ring1B 4 days after treatment under proliferation conditions (<5% of cells were immunoreactive for Ring1B). Scale bars = 100 microns **(A)**, 45 microns **(C)**.

in vitro to neuronal and glial derivatives. Typically, neurosphere cultures are established from embryonic brain regions or from the adult subventricular zone and the OB [31, 41]. To investigate the role of Ring1B in NSC self-renewal, we isolated cells from the embryonic OB that are known to show multipotential and self-renewing capacities under clonal analysis conditions. These cells reside in the proliferating layers (neuroepithelial zone) of the OB and express Ring1B (Fig. 1A). We dissected the OB from 13.5 dpc fetuses homozygous for a floxed Ring1B ($Ring1B^f$) allele that can be inactivated by Cre-mediated recombination, a strategy needed to circumvent the embryonic lethality of Ring1B inactivation [28, 42]. This *Ring1B* mutant allele was obtained by homologous recombination of a targeting construct in which *loxP* sequences flank the first coding exon of the *Ring1B* gene and a selectable *neo* cassette (Fig. 1B) [28]. These fetuses also ubiquitously expressed a cytoplasmic Cre recombinase–estrogen receptor fusion protein (Cre-ERT2) whose activity is controlled by translocation to the cell nucleus induced by 4-hydroxy-tamoxifen (4HT) [43] (Fig. 1B). NSCs were expanded in the presence of growth factors, EGF and FGF-2, and cultured in neurosphere-forming conditions, as previously described [33]. To obtain Ring1B-deficient progenitors, we treated parallel cultures seeded at 5,000 cells/cm^2 with 800 nM 4HT in ethanol, or with only vehicle, for 18 hours and scored the resulting neurospheres 72 hours later. At this stage, 4HT treatment resulted in Ring1B-depleted cell cultures, as shown by Western blot and Ring1B immunofluorescence analysis (Fig. 1C, supporting information Fig. 1A). We termed

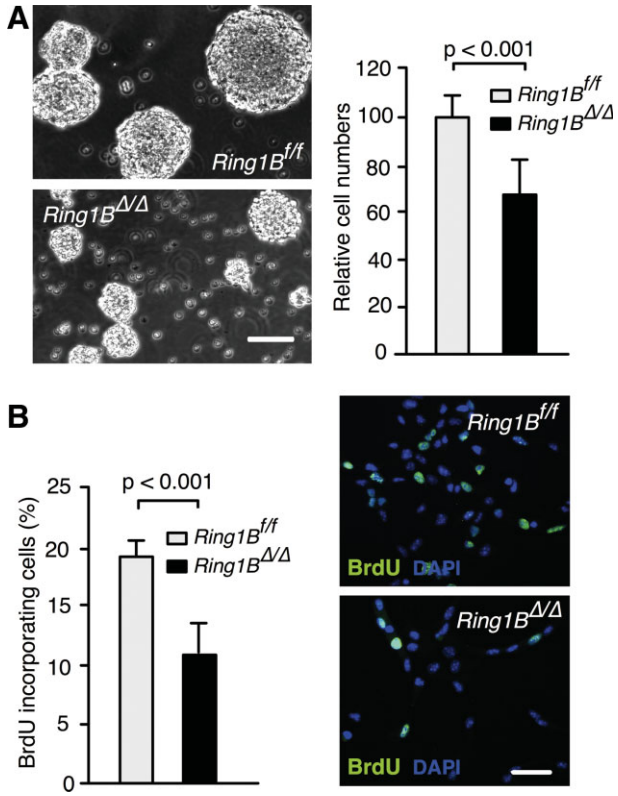

Figure 2. Impaired proliferation of *Ring1B* mutant olfactory bulb stem cells in neurosphere assays. **(A):** *Ring1B* mutant cultures show less sphere formation (left) and a lower total number of cells (right, $n = 24$). **(B):** The number of cells incorporating 5′-bromo-2-deoxyuridine (BrdU) (left, $n = 7$), as assessed by immunofluorescence analysis (right), was significantly lower in $Ring1B^{\Delta/\Delta}$ cultures than in control cultures. Error bars depict the standard error of the mean. Scale bar = 100 microns **(A)**, 45 microns **(B)**.

4HT-treated and ethanol-treated cultures as $Ring1B^{\Delta/\Delta}$ and $Ring1B^{f/f}$, respectively. $Ring1B^{\Delta/\Delta}$ cultures consisted of neurospheres whose size was smaller than that of wild-type neurospheres (Fig. 2A, left, and also the clonal analysis in Fig. 3). This observation was consistent with a poorer expansion of Ring1B-deficient cells, as indicated by the total number of cells in mutant versus wild-type cultures under proliferating conditions (Fig. 2A, right). To eliminate the possibility that transient nuclear activity of the recombinase Cre had a toxic effect on cell growth, we characterized the proliferative properties of neurospheres derived from *Cre-ERT2::Polr2a* mice and found that the proportion of BrdU-incorporating cells in tamoxifen-treated cultures was similar to that in control, ethanol-treated cultures (supporting information Fig. 1B). We also investigated the possible role of 4HT treatment characterizing neurosphere cultures from OB cells isolated from wild-type mice and found them to be indistinguishable from vehicle-treated neurospheres in cell proliferation assays (supporting information Fig. 1C). Thus, these experimental conditions had no effect on the observed results and, therefore, we conclude that the appropriate proliferation of neural stem/progenitors depends, in a cell-autonomous manner, on the activity of *Ring1B*. We then studied whether the decrease in cell numbers in mutant cultures was due to differences in apoptosis or in proliferative rates. The TUNEL analysis showed almost no apoptotic cells in either culture (0.3% and 0.2% of total cells in $Ring1B^{\Delta/\Delta}$ cultures and wild-type cultures, respectively; data not shown). In contrast, quantitation cultures that were BrdU pulsed for 1 hour demonstrated that 4HT-treated cultures contained fewer cells that had incorporated BrdU (19%) than cultures treated with ethanol (12%; $p < .005$) (Fig. 2B). To see whether this observation on OB-derived NSCs could be generalized to NSCs from other regions of the central nervous system, we investigated the proliferative properties of neurospheres derived from the cortex and ganglionic eminences of 13.5 dpc embryos. The results (supporting information Fig. 2) showed that, in the absence of Ring1B, neurosphere formation and proliferation, assessed as BrdU incorporation, were lower than in $Ring1B^{f/f}$ cultures. Collectively, these results show that defective expansion of mutant neural stem/progenitors results from a decrease in the proliferative rate of Ring1B-deficient cells.

Defective Self-Renewal of Ring1B-Deficient NSCs

The nonclonal neurosphere assay assesses the presence of NSCs but it does not inform on their self-renewal capacity. Instead, self-renewal is usually analyzed by the ability of single cells to reform spheres while retaining the production of neurons and glia. To determine whether Ring1B plays a role in NSC self-renewal, we quantitated the number of cells able to reform neurospheres when cultured as single cells. First, we treated single cell cultures with 4HT and cultured them for 7-9 days to obtain primary $Ring1B^{\Delta/\Delta}$ neurospheres (Fig. 3A, top). Efficient inactivation of Ring1B in these cultures was assessed by PCR analysis of single spheres (supporting information Fig. 3A). Second, we set up single-cell cultures from neurospheres derived from Ring1B-deficient cells to derive mutant secondary neurospheres (Fig. 3A, bottom). We also tried to establish neurospheres from two stages of single-cell cultures, but under these conditions no neurospheres were obtained from mutant OBSCs (supporting information 3B, 3C). The assays revealed that the capacity of $Ring1B^{\Delta/\Delta}$ cells to give rise to primary neurospheres was one third lower ($p < .001$) than that of wild-type cells, and that such a capacity was further reduced in secondary neurospheres, to only one fifth of that of wild-type cells ($p < .001$) (Fig. 3B). Sizes of primary and secondary mutant neurospheres from the clonal analysis were, as already seen in nonclonal neurosphere assays, smaller than those of wild-type cells (46% and 63% of that of wild-type spheres) (Fig. 3D, 3E). The comparison of neurosphere sizes obtained in these clonal assays showed a distinctive distribution in which wild-type cells generated neurospheres in the range of 200-1,800 microns in diameter, whereas mutant cells never reached diameters >800 microns (Fig. 3C). Altogether, the data show that Ring1B is required for self-renewal and proliferation of OB stem cells.

Premature Differentiation of Ring1B-Deficient NSCs

To address whether the impaired proliferation and self-renewal abilities of mutant NSCs is related to Ring1B regulation of differentiation, we evaluated the potential of E13.5-derived OB neurospheres to generate the three major neural cell lineages normally found when they are cultured under differentiation conditions, without mitogens. We found that both Ring1B-deficient and wild-type cultures formed similar numbers of neurons (Tuj1 immunoreactive cells) and astrocytes (GFAP immunoreactive cells), as shown in Figure 4. In contrast, we found a consistently lower number of oligodendrocytes (O4 immunoreactive cells) in cultures that lacked Ring1B. We tested the possibility that mutant cells were counterselected during their time in culture by identifying Ring1B-expressing cells with anti-Ring1B antibodies in cultures undergoing differentiation. The results (supporting information Fig. 4A) showed that, whereas all cells in control

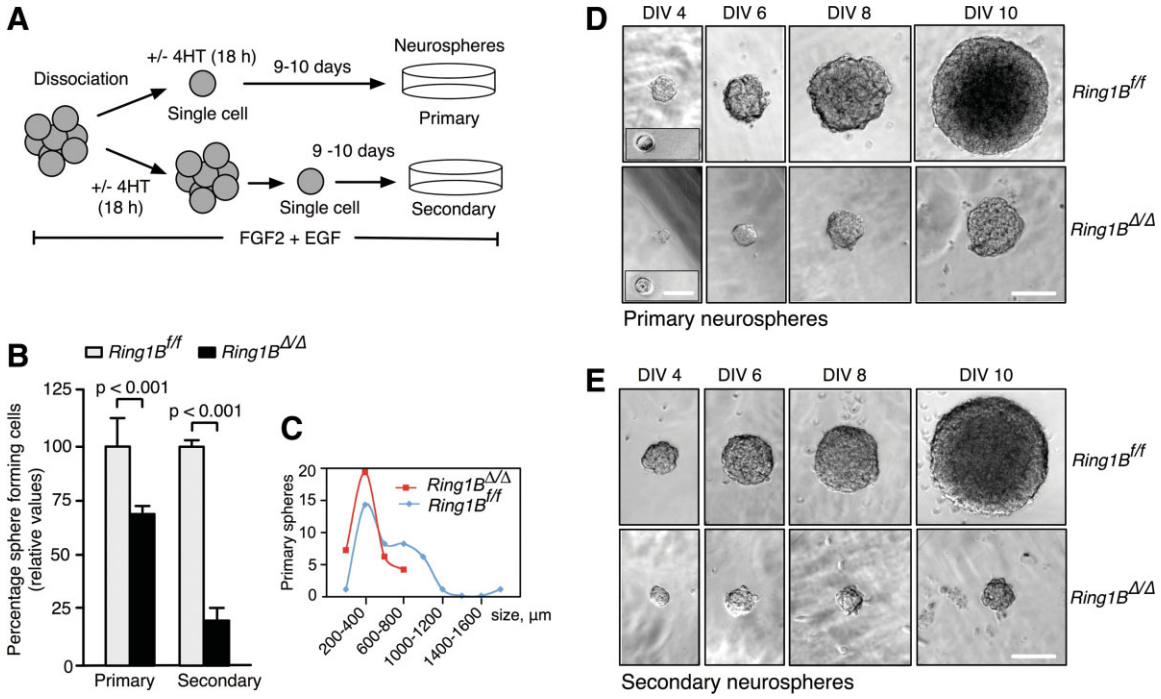

Figure 3. Ring1B deletion reduces the self-renewal capacity of olfactory bulb stem cells. **(A):** Schematic diagram of clonal analysis protocols to obtain primary and secondary *Ring1B*$^{\Delta/\Delta}$ spheres. In the first protocol (upper), 4-hydroxy-tamoxifen (4HT) was added to the cultures 18 hours before plating single cells and sphere formation was scored after 9 days in culture. In the second protocol (bottom), 4HT was added at the time of plating cells at a density of 5,000 cells/cm^2, to allow the formation of *Ring1B*$^{\Delta/\Delta}$ primary spheres. Four days after 4HT addition, primary spheres were disaggregated and plated as single cells. *Ring1B*$^{\Delta/\Delta}$ secondary sphere formation was also scored after 9 days in culture. **(B):** The percentages of single cells forming primary and secondary spheres were significantly lower, by 28% ($n = 3$ experiments; $p < .001$) and 75% ($n = 2$ experiments; $p < .001$), respectively, in *Ring1B* mutant cultures. **(C):** Distribution of the number of primary *Ring1B*$^{\Delta/\Delta}$ neurospheres versus their diameter, showing that, in mutant cultures, most spheres were smaller in size compared with controls. After 9 days in culture, the average sizes of primary spheres were 602.6 ± 54.5 microns and 326.6 ± 24.2 microns for control and *Ring1B*$^{\Delta/\Delta}$ cultures, respectively; for secondary spheres, values of average sizes were 725.3 ± 51.2 microns and 271.2 ± 32.3 microns for the control and mutant cultures, respectively. Total numbers of clonal spheres analyzed were 83 primary and 44 secondary control spheres and 70 primary and 12 secondary *Ring1B*$^{\Delta/\Delta}$ spheres. **(D, E):** Primary and secondary neurosphere cultures showing representative spheres throughout the indicated times in culture (DIV, days in vitro) after seeding single cells (inset). Scale bar for single cells, 25 microns; clonal spheres, 80 microns. Error bars depict the standard error of the mean.

cultures were stained for Ring1B, 4HT-treated cultures lacked Ring1B immunoreactivity. Because the differentiation potential of NSCs can change with developmental time, we also addressed the phenotype of neurospheres derived from 18.5 dpc OBs. Similarly to observations for Ring1B-deficient 13.5 dpc NSCs, mutant 18.5 dpc OBSCs showed impaired neurosphere formation and decreased proliferation (supporting information Fig. 5A), compared with that of untreated cultures. In the absence of growth factors, both 4HT-treated or untreated cultures generated similar proportions of the three cell lineages, although a (statistically not significant) trend toward a lower number of oligodendrocytes was observed for *Ring1B*$^{\Delta/\Delta}$ cultures (supporting information Fig. 5B). Considering that most differentiated derivatives from wild-type cells are neurons and astrocytes, the overall differentiating potential of Ring1B-deficient cells growing under nonclonal conditions was similar to that of *Ring1B*$^{f/f}$ cells after induction of differentiation. To better ascertain the differentiation potential of mutant stem cells, single cell–derived neurospheres were induced to differentiate, revealing a lower (30% of that of *Ring1B*$^{f/f}$ cells) number of tripotent clonal neurospheres (Fig. 4C, 4D). Also, the overall differentiation potential of mutant clonally derived neurospheres was lower (50% of that of *Ring1B*$^{f/f}$ cells).These findings unveil a defective differentiation potential of *Ring1B*$^{\Delta/\Delta}$ OBSCs that was masked under nonclonally derived neurospheres in nonclonal neurosphere cultures.

We next asked whether Ring1B might play a role in maintaining neural stem/progenitor cells undifferentiated, as has been observed in ES cells [15, 44]. To this end, we analyzed 4HT-treated and untreated OB stem cell cultures growing in the presence of mitogens for the expression of the neuronal differentiation marker β-tubulin III (Tuj1). We found that *Ring1B*$^{\Delta/\Delta}$ cultures contained a larger fraction (13%) of immunoreactive cells than wild-type cultures (1.4%) (Fig. 5A), suggesting that Ring1B deficiency leads to a weakened stability of the undifferentiated state of mutant cells. If, indeed, Ring1B is playing a role in the maintenance of the undifferentiated state, we reasoned that a differentiated phenotype would be better observed in stem/progenitor cells derived from compound mutant embryos in which both *Ring1B* and its paralog *Ring1A* are inactivated. Figure 5B shows that more than one third of *Ring1A*$^{-/-}$*Ring1B*$^{\Delta/\Delta}$ OB stem/progenitor cells growing in the presence of FGF and EGF-2 were immunoreactive for Tuj1, compared with <1% among those in single *Ring1A* mutant cell cultures. In addition, examples of cells possessing clear neuronal morphologies could be seen among Ring1A- and Ring1B-lacking cultures (Fig. 5B, inset). This was corroborated by double immunostaining of TuJ1$^+$ cells with Map2ab or NF-m, neuronal markers that label dendrites

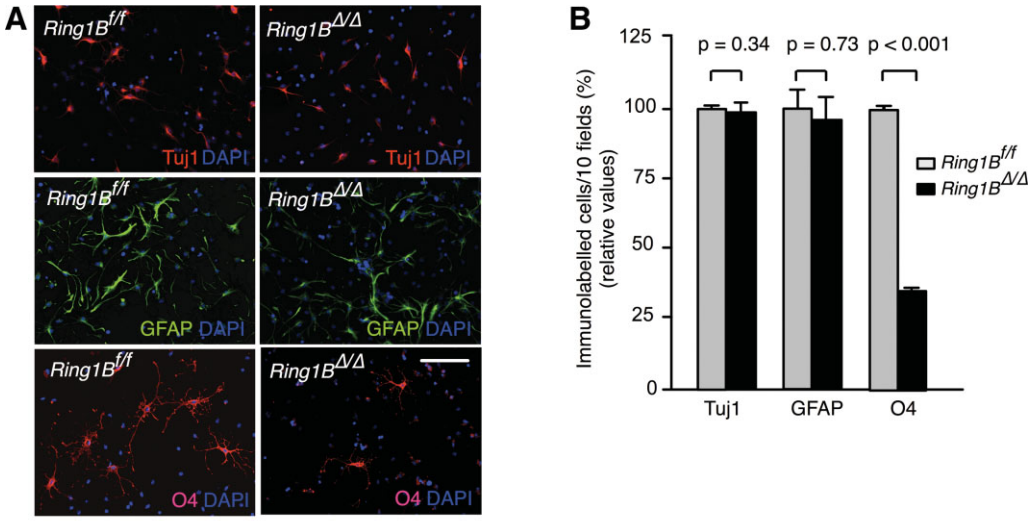

	NAO	N	A	NO	NA	Undiff.
Ring1B$^{f/f}$	57.9	5.3	10.5	5.3	0	21
Ring1B$^{\Delta/\Delta}$	17.6	11.8	0	5.9	11.8	52.9

Figure 4. Differentiation of olfactory bulb stem cells to neurons, astrocytes, and oligodendrocytes after mitogen removal. **(A):** Morphology and immunofluorescence analysis of differentiation markers in wild-type and Ring1B-deficient neural progenitors cultured for 4 days in the absence of growth factors. **(B):** Quantitation ($n = 6$) of cell lineages identified by Tuj1 (neurons), GFAP (astrocytes), and O4 (oligodendrocytes). Whereas the proportions of neurons and astrocytes were similar between wild-type and mutant cultures, Ring1B-deficient oligodendrocytes were found at a lower (one third) frequency than in wild-type cultures. Error bars depict the standard error of the mean. **(C):** Quantitation, as a percentage, of cell lineages identified in the differentiation of clonally derived neurospheres from control (20 clones) and mutant (17 clones) cultures showing tripotent (NAO), bipotent (NO, NA), and unipotent clones (N, A). **(D):** Morphology and immunofluorescence analysis of differentiation markers in representative tripotent clones of control and mutant cultures. Scale bars = 55 microns **(A)**, 50 microns **(D)**. Abbreviations: A, astrocytes; DAPI, 4′,6-diamino-2-phenylindole; GFAP, glial fibrillary acidic protein; N, neurons; O, oligodendrocytes; undiff., clones that did not express any of the differentiation markers.

and axons, respectively (Fig. 5C, 5D). Neuronal differentiation of *Ring1B*$^{\Delta/\Delta}$ stem/progenitor cells, however, was not accompanied by glial differentiation, assessed as GFAP immunoreactive cells (data not shown). Differentiation, in the absence of mitogens, of *Ring1A*$^{-/-}$*Ring1B*$^{\Delta/\Delta}$ OB stem/progenitor cells, showed a pronounced phenotype with neurons possessing long processes, fewer astrocytes and the absence of oligodendrocytes (supporting information Fig. 6). Together, the results suggest that Ring1B (and Ring1A) contribute to the stability of the undifferentiated state of neural stem/progenitor cells.

Gene Expression Analysis of Ring1B-Deficient OBSCs

Genome-wide mRNA profiling of OB-derived neurospheres under proliferating conditions by microarray analysis showed 972 probes derepressed or repressed more than twofold in *Ring1B*$^{\Delta/\Delta}$ cultures compared with control spheres. GO analysis showed an enrichment of categories related to neuronal differentiation and to cell proliferation (Fig. 6A, supporting information Table 1). For instance, Neurod1, a transcription factor specific for neurogenesis [45], Tubb3, the Tuj1 antigen, and Ina (internexin neuronal intermediate filament protein, alpha), well-known markers of neuronal differentiation, were among the genes derepressed in Ring1B-deficient cells. Also, effectors of the Notch signaling pathway, such as Hes5, were repressed in mutant cells, which is consistent with previous observations showing the large impact that their inactivation has on the self-renewal of NSCs [46, 47]. Among cell cycle regulators, Cdkn1a, an inhibitor of cyclin-dependent kinases (CDKs), which regulate progression through the G_1 phase of the cell cycle [48], was the one more clearly derepressed. To validate the microarray analysis data, we carried out QPCR on a number of select targets (Fig. 6B). Among transcriptional regulators with relevance in neural progenitor differentiation, we studied *Neurod1*, *Eomes*/*Tbr2*, *Id4*, *Prdm16*, *Ascl1*/*Mash1*, *Zfhx3*/*Atbf1*, and *Nr2f2*, all of which were upregulated in mutant neurosphere cultures, except *Ascl1*/*Mash1*. Genes encoding neuron-specific filaments, *Tubb3* and *Ina*, were also derepressed. Of the CDK-encoding genes analyzed (data not shown for *Cdkn1c*/*p57*, *Cdkn2b*/*p15*, and *Cdkn2c*/*p18*), only *Cdkn1a*/*p21* was confirmed to be upregulated. Finally, transcripts for the Notch effectors, *Hes5*, *Hes1*, and *Hey1*, were found to be repressed in an RT-QPCR analysis of Ring1B-deficient neurosphere cultures (Fig. 6B). These data show that, in the absence of Ring1B, neural progenitors upregulate an inhibitor of cell cycle progression, attenuate Notch signaling, and cannot maintain their undifferentiated state, all of which can contribute to the impaired self-renewal and reduced proliferation abilities observed in Ring1B-deficient OB stem/progenitor cells.

Considering that Ring1B is a transcriptional repressor, it appears likely that repressed genes in mutant cells are indirect targets of Ring1B. To distinguish between direct (Ring1B bound) and indirect (not Ring1B bound) targets, we used a

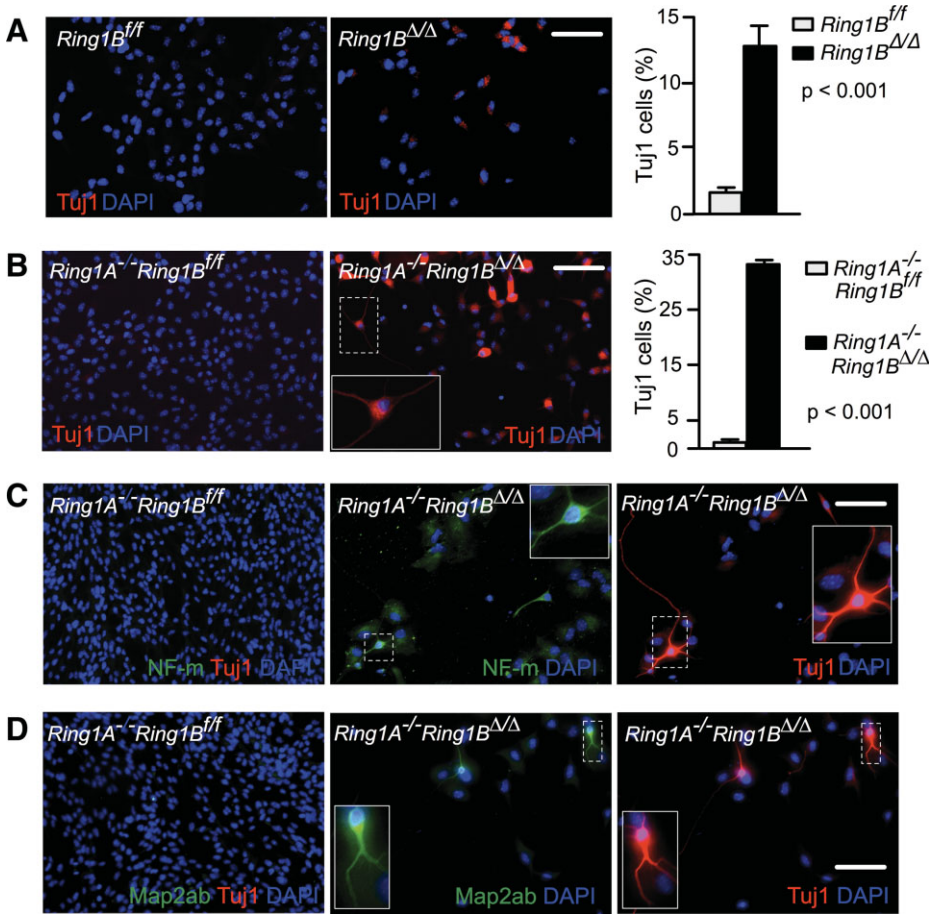

Figure 5. Accelerated neuronal differentiation in Ring1B-deleted olfactory bulb stem cells grown in the presence of mitogens. **(A):** Ring1B-deficient cultures contained a subpopulation of Tuj1$^+$ cells ($n = 6$; $p < .001$), suggesting premature differentiation even under proliferative conditions. **(B):** Unscheduled differentiation was enhanced by the inactivation of both Ring1A and Ring1B, leading to the expression of Tuj1 by one third of the cells ($n = 3$; $p < .001$), of which some possessed prominent neurites (inset). **(C, D):** Compound *Ring1A* and *Ring1B* mutant cultures stained with neuronal differentiation markers (NF-m and Map2ab). Representative fields showing cells that express both Tuj1 and NF-m **(C)** or Tuj1 and Map2ab **(D)** in the presence of mitogens. Scale bars = 50 microns. Abbreviations: DAPI, 4′,6-diamino-2-phenylindole; Map2ab, microtubule-associated protein 2ab; NF-m, neurofilament medium chain.

chromatin immunoprecipitation (ChIP) on chip approach. Supporting information Figure 7A shows the results on a subset of chosen genes. Whereas the promoter regions of a number of genes derepressed in *Ring1B*$^{\Delta/\Delta}$ cultures were bound by Ring1B (*Neurod1*, *Id4*, *Eomes*, *Prdm16*, *Nr2f2*), other upregulated loci (*Tubb3, Ina, Atbf1*, or *Cdkn1a*) showed very little bound Ring1B, suggesting that their derepression is secondary to *Ring1B* inactivation. Of interest is the fact that despite Ring1B occupancy of promoter regions of *Neurog1* and *Neurog2*, two important regulators of neural development, their expression was found unaltered in Ring1B-deficient cells. On the other hand, no Ring1B was found recruited to the chromatin of genes encoding Notch pathway members, such as *Hes1*, *Hes5*, *Hey1*, and *Dll3* (supporting information Fig. 7A), all of which were repressed in Ring1B-deficient neurospheres.

Analysis of chromatin modifications by ChIP analysis on select targets (supporting information Fig. 7B) revealed increases in the promoter proximal levels of H3K4me3, a histone marker typically associated with transcriptional activation in mutant cells. Levels of H3K27me3, a histone marker usually associated with transcriptional repression, however, showed little variation between mutant and control cultures. On the other hand, *Ring1B* inactivation lead to only a partial reduction in global levels of monoubiquitylated histone H2A (supporting information Fig. 7C), and complete depletion was only observed when both Ring1A and Ring1B were deleted (supporting information Fig. 7C). The data suggest that gene expression changes in directly regulated Ring1B targets are accompanied by chromatin modifications and that Ring1A partially compensates for the absence of Ring1B in mutant neurosphere cultures. Overall, the data suggest that Ring1B contributes to the maintenance of self-renewal and modulation of developmental potential of OBSCs throughout an intricate network of regulatory events that may be under both direct and indirect control by Ring1B.

In Vivo Altered Proliferation/Differentiation of Neural Progenitors in *Ring1B* Mutant Embryos

To assess the impact of Ring1B inactivation in an in vivo setting, we analyzed fetuses 4 days after tamoxifen treatment of gestating females, of which some received a dose of BrdU 4 hours before perfusion. For these experiments, we used *Ring1B*$^{f/f}$ females that were mated to *Ring1B*$^{f/f}$, *Rosa26::-CreERT2* males, so that mutant (Cre-expressing) and wild-type (without the Cre-expressing transgene) embryos were obtained in the same litter. Efficient Ring1B inactivation assessed by immunohistochemistry is shown in supporting information Figure 4B. Proliferation was evaluated by staining with an antibody that recognizes the phosphorylated form (at serine 10) of histone H3 (PH3), a mitotic marker. We found a lower number of labeled cells (54.5%; $p < .001$) (Fig. 7A), which agrees with the reduced proliferation seen in neurosphere assays. These PH3$^+$ cells expressed nestin (supporting information Fig. 8), indicating their neural stem/progenitor nature. The numbers of PH3$^+$ cells were also lower (25% lower than in controls; $p < .05$) in the cortex of *Ring1B*$^{\Delta/\Delta}$ 17.5 dpc fetuses (sections, $n = 16$ from two animals of each genotype). This reduction in mitotically active cells was still more

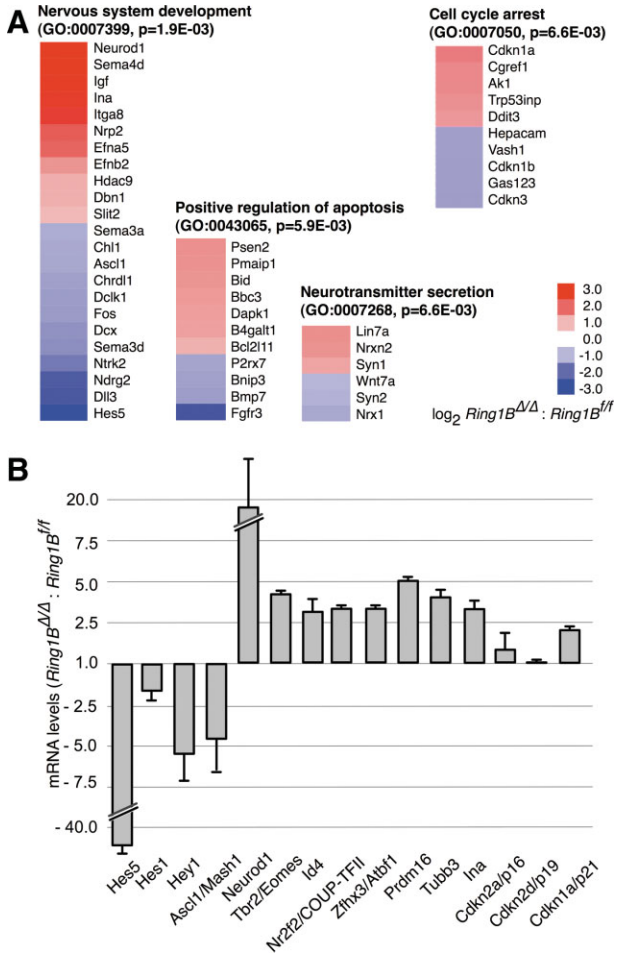

Figure 6. RNA profiling analysis of Ring1B-deleted neurospheres. **(A):** Gene ontology (GO) analysis of genes whose expression changed more than two-fold in neurosphere cultures of olfactory bulb stem cells isolated from 13.5 days postcoitum (dpc) *Ring1B*$^{f/f}$ mouse embryos, 4 days after 4-hydroxy-tamoxifen (4HT) treatment. The four most significantly altered GO categories (biological process) by statistical analysis are shown. **(B):** Validation of Ring1B target genes indicated by analysis of RNA expression profiling, using quantitative polymerase chain reaction. Changes in expression levels are displayed as the ratio between normalized (for β-actin expression) levels of select transcripts in Ring1B-deficient and wild-type neurosphere cultures. Error bars depict the standard error of the mean between three experiments. Expression analysis of the same subset of Ring1B target genes was also carried out with Ring1B-deficient neurospheres grown under differentiating conditions, with 13.5 dpc dissected olfactory bulb tissue and with *Ring1A* and *Ring1B* compound mutant neurospheres grown under proliferating conditions (supporting information Table 2).

pronounced in 17.5 dpc *Ring1A*$^{-/-}$*Ring1B*$^{\Delta/\Delta}$ embryos than in controls (supporting information Fig. 9).

We also analyzed differentiation in *Ring1B*$^{\Delta/\Delta}$ embryos. Gliogenic differentiation was analyzed in 17.5 dpc embryos, at the beginning of astrocyte formation in the developing embryo. The sections, stained with an anti-GFAP antibody, showed a lower number of stained cells in mutant embryos than in wild-type embryos (41% of those in wild-type embryos; $p < .001$) (Fig. 7B). In addition, using an alternative assay that allows the identification of differentiating, unexpanded, progenitors (32), we found a 50% lower ($p < .05$) number of GFAP$^+$ cells in 17.5 dpc mutant OBs, compared with controls ($n = 9$ control cultures and $n = 7$ *Ring1B*$^{\Delta/\Delta}$ cultures). In contrast, neurogenesis, assessed by immunostaining with anti-Tuj1 antibodies, was found to be augmented in mutant OBs, which showed greater numbers of Tuj1$^+$ cells (Fig. 7C, 7D). To test if the increase in TuJ1$^+$ cells and the reduction in GFAP$^+$ cells were due to changes in the proliferation of OB progenitor cells in vivo and/or to an increased tendency of progenitors towards neurons, dividing cells were labeled with BrdU and their differentiation was examined 4 hours later. As seen in Figure 7D and 7E, the number of BrdU$^+$ cells was 50% lower in sections from mutant embryos, whereas the fraction of BrdU$^+$ cells that expressed TuJ1 was significantly greater than that of control embryos, suggesting that neuronally biased differentiation may be responsible for the lower numbers of GFAP$^+$ cells. A similar analysis to identify doubly BrdU$^+$ and GFAP$^+$ cells could not be done because the acid treatment of sections needed to detect BrdU interferes with the weak GFAP immunostaining of sections at this developmental stage. The impaired proliferation of neural progenitors in mutant embryos, the augmented neuronal generation, and the decreased glial differentiation establish Ring1B as a promoter of proliferation of embryonic neural progenitors and as a modulator of their differentiation potential in the developing OB.

Discussion

Self-renewal of stem cells involves the coordination of signaling pathways that ensure cell replication while maintaining their differentiating potential. We report here that inactivation of Polycomb subunit Ring1B impairs proliferation and self-renewal of embryonic OB neural stem/progenitor cells, concurrently with the loss of developmental potential and accelerated neuronal differentiation. Our observations suggest that the self-renewing function of embryonic neural stem/progenitor cells uses Polycomb epigenetic regulation to balance cell cycle control and differentiation commitment.

Self-Renewal and Proliferation

Major differences between the self-renewal dynamics of embryonic/fetal and adult stem cells lie in their programs of proliferation control [4]. Thus, fetal stem cells proliferate actively and expand their populations throughout development, whereas proliferation of adult stem cells is tightly regulated, dividing rarely, as demanded by tissue homeostasis. The Polycomb role in self-renewal of NSCs is mostly known through the analysis of *Bmi1*-mutant adult mice, which show a lower number of neural stem/progenitor cells whose self-renewal ability is also impaired. These defects are thought to result from premature senescence induced by the accumulation of products of the *Ink4a* locus, which is normally repressed by Bmi1 [23–25], that are responsible for decreased neurogenesis during ageing [49].

Our studies on neural embryonic stem/progenitor cells show that their proliferation, both in neurosphere assays and in the OB, depends, at least in part, on Ring1B. Furthermore, self-renewal, as assessed in secondary neurospheres under clonogenic conditions and in two stages of single cells, is impaired in the absence of Ring1B. These results are in line with those resulting from acute inactivation of Bmi1 in embryonic stem/progenitor cells expressing Bmi1 shRNAs [26]. In both cases, loss of function of either *Bmi1* or *Ring1B* (this report) leads to little or no upregulation of the products of the *Ink4a* locus. Instead, Cdkn1a/p21, an inhibitor of the CDKs that determine progression of the cell cycle through the G_1 phase, is upregulated. A difference, however, between Bmi1

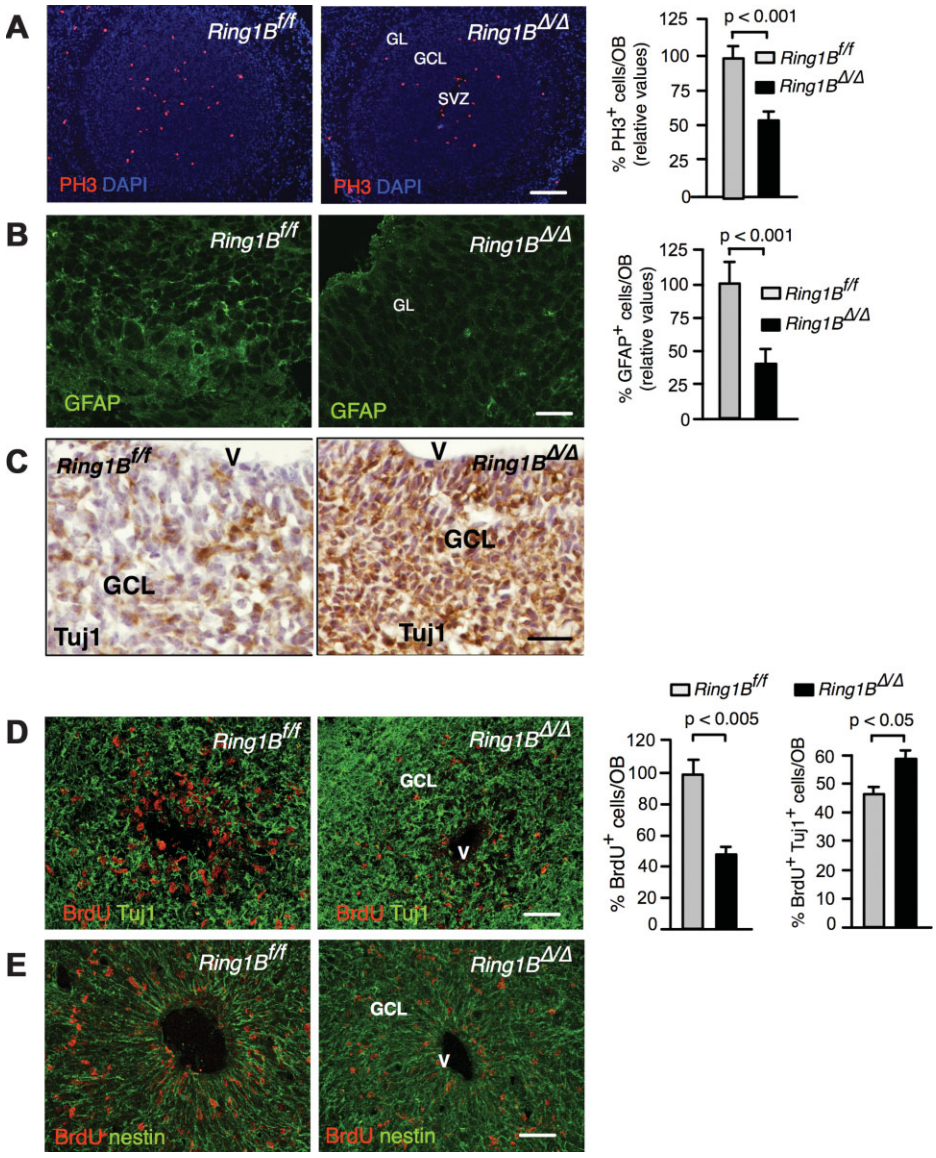

Figure 7. Proliferation and cell differentiation in the fetal OB. **(A):** Decreased cell proliferation of 17.5 dpc OBs from mice injected with tamoxifen, assessed by immunostaining with antibodies against PH3 ($n = 24$ sections from three animals of each genotype; $p < .001$). **(B):** GFAP immunostaining revealed reduced gliogenesis in 17.5 dpc Ring1B-deficient OBs ($n = 24$ sections from three animals of each genotype). **(C):** Histochemical analysis of 17.5 dpc OB, showing a higher number of Tuj1-expressing cells in the subventricular and granular cell layers of mutant OBs. **(D):** Confocal microscope images of 17.5 dpc OB sections from mice injected with BrdU 4 hours before sacrifice to identify proliferating cells (assessed by anti-BrdU immunostaining) and newly differentiating cells (immunostained with Tuj1 antibodies) from dividing progenitors ($n = 20$ sections from two mutant and two control animals). Histograms show that, in *Ring1B*$^{\Delta/\Delta}$ OBs, a significant fraction of proliferating cells had begun to differentiate into neurons (right) despite the generalized decrease in cell proliferation in the mutant OB (left). **(E):** Confocal microscope images of neural progenitors (nestin-expressing cells) in 17.5 dpc OBs from mice injected with BrdU 4 hours before sacrifice, showing the lower proliferative rate in mutant OBs. Scale bars = 100 microns **(A)**, 20 microns **(B)**, 25 microns **(C)**, and 38 microns **(D, E)**. Abbreviations: BrdU, 5′-bromo-2-deoxyuridine; DAPI, 4′,6-diamino-2-phenylindole; dpc, days postcoitum; GCL, granule cell layer; GFAP, glial fibrillary acidic protein; GL, glomerular layer; OB, olfactory bulb; PH3, phosphohistone H3; SVZ, subventricular zone.

and Ring1B activities promoting fetal NSC self-renewal appears to be suppressing apoptotic programs, which seems to depend more on Bmi1 [26] than on Ring1B, given the indistinguishable apoptotic rates of wild-type *Ring1B* mutant progenitors. In this regard, it seems peculiar that a set of deregulated genes in Ring1B-deficient OB-derived neurospheres belongs in the GO term of positive regulation of apoptosis. On the other hand, negative regulation of Cdkn1a/p21 by Polycomb products may occur through indirect mechanisms because, at least for Ring1B, we found no evidence of association with gene promoter regions. Cell cycle control of adult neural stem/progenitor cells is controlled, at least in part, by CDKIs encoded by *Ink4a* and *Cdkn1a/p21* [24, 50, 51]. However, our data, together with previous observations such as the growing impact of Bmi1 inactivation on self-renewal of developing neural progenitors while

Cdkn1a/*p21* upregulation decreases over time [26] and the lack of *p16Ink4a* upregulation in the fetal brain from *Bmi1*$^{-/-}$ mice [24] and fetal *Ring1B*$^{\Delta/\Delta}$ OB-derived neurospheres (Fig. 7B), suggest that negative regulation of *Cdkn1a*/*p21* is a prevalent mechanism during expansion of embryonic neural stem/progenitor cells.

Maintenance of Differentiation Potential

Our striking observation that Ring1B-deficient embryonic neurospheres growing under proliferative conditions express differentiation markers (β-tubulin III) suggests defective maintenance of the undifferentiated state central to stem/progenitor cells. Unscheduled differentiation in the absence of Ring1B was, however, only partial, because when its paralog, Ring1A, was also inactivated, signs of differentiation affected a larger fraction of cells in the culture, some of which expressed morphological features of neurons and expressed not only β-tubulin III but also neuronal markers characteristic of differentiated neurons, such as Map2ab and neurofilament. Nevertheless, Ring1B-deficient neurospheres derepress a number of transcription factors relevant to the differentiation of neural progenitors and the specification of neuronal fates, in particular, *Neurod1*, which appear as Ring1B direct targets. Acute inactivation of *Bmi1*, in contrast, does not lead to similar differentiative defects, although downregulation of progenitor markers such as Nestin and Neurog2 were observed [26]. It is worth noting that the fewer GFAP$^+$ cells and the lack of O4$^+$ cells together with the presence of large process-bearing Tuj1$^+$ cells in Ring1A- and Ring1B-deficient cells growing without mitogens suggest that neuronal differentiation is much favored in these mutant progenitors. Most likely this relates to the observation that the neural cell fate appears to be the default specification during neural differentiation [52, 53]. The accelerated neuronal differentiation seen here in Ring1A- and Ring1B-deficient neural progenitors parallels the differentiative defects seen in Ring1B-deficient ES cells [44, 54], except for the fact that the failure to prevent differentiation leads toward a defined, rather than a more disordered, cell fate, possibly due to restrictions on the developmental potential of tissue-specific stem cells.

A possible explanation for the premature differentiation of Ring1B-deficient neural progenitors is that some of the signaling pathways involved in stem cell self-renewal are affected. Of these, the Notch pathway appears to be a good candidate, considering the accelerated differentiation of NSCs defective in one or more components of the Notch signaling pathway [46, 55]. Active Notch signaling downregulates proneural gene expression, thus inhibiting neuronal differentiation (reviewed in [56–59]). Indeed, expression analysis of Ring1B-deficient neurosphere cultures, under proliferating conditions, shows that stationary mRNA levels of Notch effectors, such as Hes5, are downregulated. Considering that Ring1B is a transcriptional repressor, it is likely that downregulation of Notch effectors occurs through indirect effects, perhaps through the upregulation of uncharacterized transcriptional repressors or microRNAs. In this regard, it is worth noting that regulation of Notch target genes is preferentially modulated by postranslational modifications in subunits of transcriptional complexes, leading to the dismissal/recruiting of coactivators and corepressors [60]. Although Bmi1 and Ring1B associate with each other for efficient H2A monoubiquitylation [18, 22, 27, 61], the fact that Bmi1 inactivation does not have a similar impact on Notch signaling may be due to functional substitution by Bmi1 paralogs known to act as cofactors in H2A modification [61, 62]. Alternatively, it is possible that Ring1B complexes other than PRC1 are involved, at least in part, in transcriptional control of the regulatory network associated with the program defined by Notch signaling.

Coordinated regulation of cell cycle exit and differentiation of progenitors is essential for the generation of appropriate numbers of cells. Thus, in epithelial cells, Notch1 has been found to activate p21 expression [63]. In contrast, in our *Ring1B*$^{\Delta/\Delta}$ neural stem/progenitor cells, Notch signaling downregulation occurs with p21 upregulation. However, rather than an inconsistency, both observations may only be a reflection of the known context dependency of Notch signaling activity, by which it can serve both as an oncogene and also as a tumor suppressor [64]. In neural stem/progenitor cells, it is not known whether slowing proliferation, perhaps due to upregulation of inhibitors of cell proliferation (Cdkn1a/p21), and unscheduled differentiation are related processes or whether they are independent of each other. It has been noted that cell cycle lengthening of neural progenitors may contribute to a switch from proliferative to neuron-generating cell division [65]. If this is the case, it is conceivable that downregulation of the Notch pathway may occur as a consequence of a primary alteration in the cell cycle. This is illustrated by *Hes1* repression mediated by p107 [66], an inhibitor of G_1–S transition. Alternatively, premature neurogenesis, induced by weakening of Notch signaling, may lead, even in the presence mitogens, to slower, neurogenic-like cell divisions previous to eventual cell cycle withdrawal.

Our results show that, in the absence of mitogens, loss of function of *Ring1B* has little effect on cell differentiation under nonclonal conditions (as a fraction of neural and glial derivatives and the total number of differentiated cells). An exception is the significantly lower number of oligodendrocytes formed in *Ring1B*$^{\Delta/\Delta}$ than in control neurosphere cultures, a phenotype strongly enhanced in *Ring1A*$^{-/-}$*Ring1B*$^{\Delta/\Delta}$ mutant cultures. This observation could not be confirmed in vivo, because olidogendrocyte formation peaks postnatally and the administration of tamoxifen to gestating mice leads to defective delivery of pups (also, tamoxifen treatment at very early stages leads to a severe developmental defect in our *Ring1B* mutant mouse line). However, a similar phenotype was recently reported for neural progenitors depleted of Ezh2 (the Polycomb protein with activity of histone H3K27 methyltransferase), which were found to be unable to differentiate into oligodendrocytes [67]. In vivo, we found alterations in astrocyte and neuron differentiation in the OB. First, fewer GFAP$^+$ cells were detected in 17.5 dpc mutant fetuses that were exposed to tamoxifen at day 13.5 of development, compared with controls, suggesting defective astrocytic differentiation. In contrast, neurogenesis at the same developmental stage, assessed as Tuj1$^+$ cells, appeared enhanced. Although *Ring1B*$^{\Delta/\Delta}$ OB progenitor proliferation is lower than in controls, they contain more double Tuj1$^+$BrdU$^+$ cells, suggesting that the tendency toward neuronal differentiation of mutant progenitors may account for the lower number of GFAP$^+$ cells in mutant OBs. Finally, alterations in the differentiating ability of *Ring1B*$^{\Delta/\Delta}$ progenitors were also observed in the lower developmental potential of clonally derived mutant neurospheres.

In summary, we have shown that the Polycomb protein Ring1B promotes proliferation and self-renewal of embryonic neural stem/progenitor cells through the repression of cell cycle inhibitors and maintenance of signaling pathways (Notch) that prevent differentiation. The data also suggest that Ring1B is part of the mechanisms that regulate competence of embryonic neural stem/progenitor cells to generate neurons and glia over developmental time.

Acknowledgments

We thank Y. Mizutani and R. Varillas for excellent technical help. We thank V. Campuzano and M. Barbacid for the RERTert mouse line and M. Endoh for the *Eomes* primers and help with the ChIP experiments. T.E. acknowledges Dr. Toyoda's support. M.R-T. and H. M-G. were recipients of FPU and FPI fellowships, respectively, from the Ministerio de Educacion y Ciencia and Comunidad de Madrid, respectively. This work was supported by grants SAF2007-65957-C02-01 (M.V.), the Onco-Cycle program from the Comunidad de Madrid (M.V.), SAF2004-05798, and CIBERNED CB06/05/0065 from Instituto de Salud Carlos III (C.V-A.)

Disclosure of Potential Conflicts of Interest

The authors indicate no potential conflicts of interest.

References

1 Weissman IL. Stem cells: Units of development, units of regeneration, and units in evolution. Cell 2000;100:157–168.
2 Morrison SJ, Kimble J. Asymmetric and symmetric stem-cell divisions in development and cancer. Nature 2006;441:1068–1074.
3 Molofsky AV, Pardal R, Morrison SJ. Diverse mechanisms regulate stem cell self-renewal. Curr Opin Cell Biol 2004;16:700–707.
4 Orford KW, Scadden DT. Deconstructing stem cell self-renewal: Genetic insights into cell-cycle regulation. Nat Rev Genet 2008;9: 115–128.
5 Mimeault M, Batra SK. Concise review: Recent advances on the significance of stem cells in tissue regeneration and cancer therapies. Stem Cells 2006;24:2319–2345.
6 Kim J, Chu J, Shen X et al. An extended transcriptional network for pluripotency of embryonic stem cells. Cell 2008;132:1049–1061.
7 Niwa H. How is pluripotency determined and maintained? Development 2007;134:635–646.
8 Silva J, Smith A. Capturing pluripotency. Cell 2008;132:532–536.
9 Spivakov M, Fisher AG. Epigenetic signatures of stem-cell identity. Nat Rev Genet 2007;8:263–271.
10 Cao R, Wang L, Wang H et al. Role of histone H3 lysine 27 methylation in Polycomb-group silencing. Science 2002;298:1039–1043.
11 Wang H, Wang L, Erdjument-Bromage H et al. Role of histone H2A ubiquitination in Polycomb silencing. Nature 2004;431:873–878.
12 Levine SS, King IF, Kingston RE. Division of labor in Polycomb group repression. Trends Biochem Sci 2004;29:478–485.
13 Boyer LA, Plath K, Zeitlinger J et al. Polycomb complexes repress developmental regulators in murine embryonic stem cells. Nature 2006;441:349–353.
14 Bracken AP, Dietrich N, Pasini D et al. Genome-wide mapping of Polycomb target genes unravels their roles in cell fate transitions. Genes Dev 2006;20:1123–1136.
15 Lee TI, Jenner RG, Boyer LA et al. Control of developmental regulators by Polycomb in human embryonic stem cells. Cell 2006;125: 301–313.
16 Stock JK, Giadrossi S, Casanova M et al. Ring1-mediated ubiquitination of H2A restrains poised RNA polymerase II at bivalent genes in mouse ES cells. Nat Cell Biol 2007;9:1428–1435.
17 Wang L, Brown JL, Cao R et al. Hierarchical recruitment of Polycomb group silencing complexes. Mol Cell 2004;14:637–646.
18 Cao R, Tsukada YI, Zhang Y. Role of Bmi-1 and Ring1A in H2A ubiquitylation and Hox gene silencing. Mol Cell 2005;20:845–854.
19 Schoeftner S, Sengupta AK, Kubicek S et al. Recruitment of PRC1 function at the initiation of X inactivation independent of PRC2 and silencing. EMBO J 2006;25:3110–3122.
20 Valk-Lingbeek ME, Bruggeman SW, Van Lohuizen M. Stem cells and cancer; the Polycomb connection. Cell 2004;118:409–418.
21 Mohn F, Weber M, Rebhan M et al. Lineage-specific Polycomb targets and de novo DNA methylation define restriction and potential of neuronal progenitors. Mol Cell 2008;30:755–766.
22 Li Z, Cao R, Wang M et al. Structure of a Bmi-1-Ring1B Polycomb group ubiquitin ligase complex. J Biol Chem 2006;281:20643–20649.
23 Bruggeman SW, Valk-Lingbeek ME, van der Stoop PP et al. Ink4a and Arf differentially affect cell proliferation and neural stem cell self-renewal in Bmi1-deficient mice. Genes Dev 2005;19:1438–1443.
24 Molofsky AV, Pardal R, Iwashita T et al. Bmi-1 dependence distinguishes neural stem cell self-renewal from progenitor proliferation. Nature 2003;425:962–967.
25 Molofsky AV, He S, Bydon M et al. Bmi-1 promotes neural stem cell self-renewal and neural development but not mouse growth and survival by repressing the p16Ink4a and p19Arf senescence pathways. Genes Dev 2005;19:1432–1437.
26 Fasano CA, Dimos JT, Ivanova NB et al. shRNA knockdown of Bmi-1 reveals a critical role for p21-Rb pathway in NSC self-renewal during development. Cell Stem Cell 2007;1:87–99.
27 Buchwald G, van der Stoop P, Weichenrieder O et al. Structure and E3-ligase activity of the Ring-Ring complex of Polycomb proteins Bmi1 and Ring1b. EMBO J 2006;25:2465–2474.
28 Calés C, Román-Trufero M, Pavón L et al. Inactivation of the Polycomb group protein Ring1B unveils an antiproliferative role in hematopoietic cell expansion and cooperation with tumorigenesis associated with Ink4a deletion. Mol Cell Biol 2008;28:1018–1028.
29 del Mar Lorente M, Marcos-Gutiérrez C, Pérez C et al. Loss- and gain-of-function mutations show a Polycomb group function for Ring1A in mice. Development 2000;127:5093–5100.
30 Mijimolle N, Velasco J, Dubus P et al. Protein farnesyltransferase in embryogenesis, adult homeostasis, and tumor development. Cancer Cell 2005;7:313–324.
31 Seibler J, Zevnik B, Küter-Luks B et al. Rapid generation of inducible mouse mutants. Nucleic Acids Res 2003;31:e12.
32 Vergaño-Vera E, Yusta-Boyo MJ, de Castro F et al. Generation of GABAergic and dopaminergic interneurons from endogenous embryonic olfactory bulb precursor cells. Development 2006;133: 4367–4379.
33 Vicario-Abejón C, Yusta-Boyo MJ, Fernández-Moreno C et al. Locally born olfactory bulb stem cells proliferate in response to insulin-related factors and require endogenous insulin-like growth factor-I for differentiation into neurons and glia. J Neurosci 2003;23: 895–906.
34 García E, Marcos-Gutiérrez C, del Mar Lorente M et al. RYBP, a new repressor protein that interacts with components of the mammalian Polycomb complex, and with the transcription factor YY1. EMBO J 1999;18:3404–3418.
35 Wu Z, Irizarry R, Gentleman R et al. A model-based background adjustment for oligonucleotide expression arrays. J Am Stat Assoc 2004;99:909–917.
36 Hijikata A, Kitamura H, Kimura Y et al. Construction of an open-access database that integrates cross-reference information from the transcriptome and proteome of immune cells. Bioinformatics 2007; 23:2934–2941.
37 Draghici S, Khatri P, Martins RP et al. Global functional profiling of gene expression. Genomics 2003;81:98–104.
38 Benjamini Y, Hochberg Y. Controlling the false discovery rate: A practical and powerful approach to multiple testing. J R Stat Soc Ser B Methodol 1995;57:289–300.
39 Wang X, Seed B. A PCR primer bank for quantitative gene expression analysis. Nucleic Acids Res 2003;31:e154.
40 Reynolds BA, Rietze RL. Neural stem cells and neurospheres—re-evaluating the relationship. Nat Methods 2005;2:333–336.
41 Gritti A, Bonfanti L, Doetsch F et al. Multipotent neural stem cells reside into the rostral extension and olfactory bulb of adult rodents. J Neurosci 2002;22:437–445.
42 Voncken JW, Roelen BA, Roefs M et al. Rnf2 (Ring1b) deficiency causes gastrulation arrest and cell cycle inhibition. Proc Natl Acad Sci U S A 2003;100:2468–2473.
43 Indra AK, Warot X, Brocard J et al. Temporally-controlled site-specific mutagenesis in the basal layer of the epidermis: Comparison of the recombinase activity of the tamoxifen-inducible Cre-ER(T) and Cre-ER(T2) recombinases. Nucleic Acids Res 1999;27:4324–4327.
44 Endoh M, Endo TA, Endoh T et al. Polycomb group proteins Ring1A/B are functionally linked to the core transcriptional regulatory circuitry to maintain ES cell identity. Development 2008;135: 1513–1524.
45 Seo S, Lim J, Yellajoshyula D et al. Neurogenin and NeuroD direct transcriptional targets and their regulatory enhancers. EMBO J 2007; 26:5093–5108.
46 Hitoshi S, Alexson T, Tropepe V et al. Notch pathway molecules are essential for the maintenance, but not the generation, of mammalian neural stem cells. Genes Dev 2002;16:846–858.
47 Ohtsuka T, Sakamoto M, Guillemot F et al. Roles of the basic helix-loop-helix genes Hes1 and Hes5 in expansion of neural stemv cells of the developing brain. J Biol Chem 2001;276: 30467–30474.

48 Sherr CJ, Roberts JM. CDK inhibitors: Positive and negative regulators of G1-phase progression. Genes Dev 1999;13:1501–1512.
49 Molofsky AV, Slutsky SG, Joseph NM et al. Increasing p16INK4a expression decreases forebrain progenitors and neurogenesis during ageing. Nature 2006;443:448–452.
50 Kippin TE, Martens DJ, Kooy DVD. p21 loss compromises the relative quiescence of forebrain stem cell proliferation leading to exhaustion of their proliferation capacity. Genes Dev 2005;19:756–767.
51 Meletis K, Wirta V, Hede S et al. p53 suppresses the self-renewal of adult neural stem cells. Development 2006;133:363–369.
52 Smukler SR, Runciman SB, Xu S et al. Embryonic stem cells assume a primitive neural stem cell fate in the absence of extrinsic influences. J Cell Biol 2006;172:79–90.
53 Tropepe V, Hitoshi S, Sirard C et al. Direct neural fate specification from embryonic stem cells: A primitive mammalian neural stem cell stage acquired through a default mechanism. Neuron 2001;30:65–78.
54 Leeb M, Wutz A. Ring1B is crucial for the regulation of developmental control genes and PRC1 proteins but not X inactivation in embryonic cells. J Cell Biol 2007;178:219–229.
55 de la Pompa JL, Wakeham A, Correia KM et al. Conservation of the Notch signalling pathway in mammalian neurogenesis. Development 1997;124:1139–1148.
56 Bertrand N, Castro DS, Guillemot F. Proneural genes and the specification of neural cell types. Nat Rev Neurosci 2002;3:517–530.
57 Kageyama R, Ohtsuka T, Hatakeyama J et al. Roles of bHLH genes in neural stem cell differentiation. Exp Cell Res 2005;306:343–348.
58 Ross SE, Greenberg ME, Stiles CD. Basic helix-loop-helix factors in cortical development. Neuron 2003;39:13–25.
59 Yoon K, Gaiano N. Notch signaling in the mammalian central nervous system: Insights from mouse mutants. Nat Neurosci 2005;8:709–715.
60 Perissi V, Scafoglio C, Zhang J, Ohgi KA, Rose DW, Glass CK, Rosenfeld MG. TBL1 and TBLR1 phosphorylation on regulated gene promoters overcomes dual CtBP and NCoR/SMRT transcriptional repression checkpoints. Mol Cell 2008;29:755–766.
61 Sánchez C, Sánchez I, Demmers JA et al. Proteomic analysis of Ring1B/Rnf2 interactors identifies a novel complex with the Fbx110/Jhdm1B histone demethylase and the Bcl6 interacting corepressor. Mol Cell Proteomics 2007;6:820–834.
62 Elderkin S, Maertens GN, Endoh M et al. A phosphorylated form of Mel-18 targets the Ring1B histone H2A ubiquitin ligase to chromatin. Mol Cell 2007;28:107–120.
63 Rangarajan A, Talora C, Okuyama R et al. Notch signaling is a direct determinant of keratinocyte growth arrest and entry into differentiation. EMBO J 2001;20:3427–3436.
64 Radtke F, Raj K. The role of Notch in tumorigenesis: Oncogene or tumour suppressor? Nat Rev Cancer 2003;3:756–767.
65 Calegari F, Huttner WB. An inhibition of cyclin-dependent kinases that lengthens, but does not arrest, neuroepithelial cell cycle induces premature neurogenesis. J Cell Sci 2003;116:4947–4955.
66 Vanderluit JL, Wylie CA, McClellan KA et al. The retinoblastoma family member p107 regulates the rate of progenitor commitment to a neuronal fate. J Cell Biol 2007;178:129–139.
67 Sher F, Rössler R, Brouwer N et al. Differentiation of neural stem cells into oligodendrocytes: Involvement of the Polycomb group protein Ezh2. Stem Cells 2008;26:2875–2883.


See www.StemCells.com for supporting information available online.